INSTITUTE OF HIGH ENERGY PHYSICS, SERPUKHOV
Report IHVE SKU 70-57

SYSTEM OF SLOW TARGETING OF AN ACCELERATED BEAM ON INTERNAL TARGETS IN THE IHEP 70 GeV ACCELERATOR

V.I. Gridasov, A.A. Kardash, K.M. Kozlov, O.V. Kurnaev,
V.V. Lapin, S.V. Lobanov, L.L. Mojzhes, K.P. Myznikov
and A.A. Naumov

Serpukhov 1970

Translated at CERN by R. Luther
(Original: Russian)
Revised by N. Mouravieff

(CERN Trans. 72-20)

Geneva
December 1972

1. Introduction

Most of the counter experiments at the IHEP accelerator involve secondary particle beams produced on internal targets. There are several targets operating in each channel and they are positioned inside the vacuum chamber in such a way that the secondary particles can be extracted into a channel over a wide momentum range and with minimum production angles. Secondary particle beams can thus be extracted with an intensity of up to 10^6 particles per pulse. In the optimum position the targets can be moved by as much as $\pm$ 5 cm along the radius from the centre of the vacuum chamber. Secondary particles are generated on the internal targets by targetting the accelerated beam on them during the flat top of the accelerator's magnetic cycle. This lasts 1,5 sec. with 4.10^{-4} stability at 12 kilooersted and at a relative value of $2-3.10^{-5}$ for ripple amplitude of the dominant frequencies 25, 50 and 150 Hz.

The intensity of the secondary particle beams can only be exploited efficiently if the extraction time is increased to the maximum and bunching in the extracted beam is eliminated. The extraction time in the IHEP accelerator is increased beyond 1 sec. by reducing the beam targetting rate to 3-5 mm/sec. At such low rates, the only way to obtain beams which are sufficiently uniform in time and to eliminate bunching due to magnet ripple is to introduce into the targetting system particle current feedback from the target.

In this case, the conventional methods of beam targetting involving variation of the R.F. accelerating cycle (viz. for example[1]) are quite unsuitable. With these systems, the beam cannot be moved $\pm$5 cm from the equilibrium orbit without causing losses in stability and the time structure cannot be eliminated in the extracted beam. The system which we shall describe for targetting an accelerated beam on internal targets is based on the artificial excitation of azimuthal asymmetry of the accelerator's magnetic field. This system differs from the existing methods[2,3] in that

the working range of the targets can thus be substantially extended along the radius and extracted beams of more than 1 sec. duration can be obtained with no more than 10 per cent bunching.

2. Peculiarities of beam motion during targetting

Paper /4/ contains a detailed calculation of the accelerated beam's dynamics during targetting on internal targets. It was established that, due to the effect of the magnetic field's non-linear components, the frequency of the radial Q_r and vertical Q_z betatron oscillations at H = 12 kilooersted, depends greatly on the radial position of the orbit. Consequently, for fixed orbit positions along the radius, both linear resonances and also resonances of higher orders may appear. This is all the more probable as, during targetting, the beam stays on the flat top of the magnetic cycle for more than one second. An experimental check has fully confirmed this proposition. Fig. 1 illustrates the behaviour of the horizontal and vertical dimensions of the beam in motion at various radii during a flat top at H = 12 kOe. The beam is lost completely when it moves 3 cm inside or 2 cm outside the central orbit. This corresponds to the calculated position of the full and parametric resonances. In the interval between these two resonances, the beam is disturbed by non-linear resonances. These may have a substantial influence on the efficiency of the beam's interaction with the target and may deteriorate the time structure of the extracted beams. For this reason, targetting techniques involving the artificial expansion (compression) of the orbit are totally unacceptable.

During targetting, it is best to keep the accelerated beam in an undisturbed region close to the central orbit and to perform the actual targetting operation without upsetting the beam's vertical and radial stability. With this in view, we selected a method involving the artificial excitation of local orbit deformations. The orbit was deformed in this way over about the half-wavelength of betatron oscillations by exciting an additional field in two magnets

which increased in time to the value $\frac{\Delta H}{H} = 3\ \%$. The shape of the deformed orbit is shown in fig. 2. Curve 1 corresponds to the deformation produced by the focussing magnets and curve 2 to that caused by the defocussing magnets. Calculations have shown that, in the case of deformations corresponding to curve 1, the frequency shift at a deformation amplitude of ± 5 cm may reach $\pm 0{,}04$ (fig. 3, 3a). When the defocussing magnets are used, the frequency shifts caused by the variations in gradient and by the non-linear field terms cancel each other out, so that the total shift becomes negligible (figs. 3, 3b). Thus, by setting up deformations in the defocussing magnets, the effective area of the targets can be extended to ± 5 cm and over.

The time structure in extracted beams with an R.F. voltage is eliminated by stopping acceleration at the moment of transition to the flat top. Targetting begins only after debunching. As the resonance effects are eliminated from the targetting process, the time structure can only be caused by magnet ripple. In order to suppress this effect efficiently, we introduced proportional feedback from the detector of beam current in the target and ensured quick action and a broad frequency range in the power supply system for the supplementary windings. On the other hand, current ripple in the power supply system itself is reduced to such a low level that it does not cause any noticeable bunching of the particle flux.

3. Description of the system

The current is fed to the supplementary windings from controlled thyristor converters powered through a three-phase bridge circuit by inductor synchro oscillators operating at 1100 Hz and 260 Kva (fig. 4). The voltage of the thyristor converter is regulated by means of negative signal feedback from a detector which records the beam current on to the target. This detector consists of a scintillation monitor designed to record the intensity of secondary particles produced on the target. Fig.5 shows a block diagram of the system for regulating the beam current

on to the target and the corresponding logarithmic frequency characteristics[5].

In order to achieve the maximum possible frequency range, which is determined by the supply voltage frequency of 1100 Hz, the time instability for the shaping of gating pulses for the thyristors is reduced to 10-20 microsec. The system uses PTL-100 avalanche thyristors with an intrinsic gating time of a few microsec. Power supply filters, which prevent any noticeable distortion of the oscillaters' sinusoidal voltage, ensure the necessary stability for linking the thyristors' control system to the moments when the 1100 Hz voltage passes through zero. "C"-type capacitors with a capacitance of several hundred microfarad., connected to the bus-bars of the oscillator voltage (fig. 4), are used as power supply filters. This leads to a considerable reduction in the load imposed on the oscillator windings by higher current harmonics caused by the operation of the inductive load converter. In order to suppress the dangerous resonance surges which may occur at the higher harmonics, "Rg" dampers of a few ohms resistance are connected in parallel with the "C" capacitors.

The transfer functions of the individual components and the whole block diagram, as shown in fig. 5, are an important feature of the system for regulating the beam current on to the target as they make it possible to deal efficiently with variations in the feed-back signal caused by the instability of the flat top and by ripple harmonics in the range 25-600 Hz.

This feature may be attributed to the uniformity of the amplification factor and to the phase shift in the above frequency band, which is close to zero due to the form of the logarithmic frequency characteristics (fig. 5). It should be noted that the use of a stepped-up power supply frequency of 1100 Hz cuts out amplitude and phase distortions during the compensation of variations in feed-back signal by the control rectifier at ripple

frequencies of the accelerator's magnetic field*.

---

* When plotting the logarithmic frequency characteristics, the components were given the following transfer functions:

a) amplification factor of the feed-back amplifier (fba)

$$K_{fba} = \frac{U\ output}{U\ input} = 2,5;$$

b) transfer function /5/ of the thyristor converter

$$K_{ctr} = \frac{U\ tc}{U\ output} = \frac{E\ tc}{U\ output}\left(\frac{1}{T_J\ p+1}\right) = 15\ \frac{1}{76.10^{-6}\ p + 1}$$

where $T_\gamma = \frac{\gamma}{2\omega_o}$

γ - is the commutation angle which is less than or equal to $\pi/3$, $\omega_o = 2\pi .1100$ - the angular frequency of the inductor oscillators, ctr is the controlled thyristor rectifier and tc is the thyristor converter;

c) the transfer function of the current derivative in the load

$$K_{ld} = \frac{pIl}{Utc} = \frac{P}{pL1 + Rl} = \frac{Klp}{Tlp + 1} = \frac{3.3p}{0.2p + 1},\ L_1 = 0.06H,$$

$R_1 = 0.3$ ohm;

where ld is the load derivative;

d) transmission factor of beam displacement versus bump current in the supplementary magnet winding

$$K_o = \frac{r}{I_1} = 0.025\ \frac{cm}{a};$$

where l is the load;

e) transfer function of the secondary particle intensity monitor

$$K_{mon} = \frac{U_{mon}}{p\,\eta} = 32\ \frac{V/cm}{sec.}$$

where η is the radius
(at a beam current on to the target of 10^{12} $\frac{protons}{sec.}$);

f) transfer function of the open regulating system

$$K_{(r)} = K_{fba} \cdot K_{ctr} \cdot K_{ld} \cdot K_{o} \cdot K_{mon} = \frac{100 \cdot p}{(0.2p+1)\ \ (76.10^{-6}p+1)}$$

When the feedback from the beam current pickup is replaced by feedback from the magnetic current pickup in the supplementary winding (fig.4), key-stone current pulses can be shaped with a flat or sloping top and these may be used in particular for supplying beam to the target during fast spill, for correcting the orbit from section to section etc. The stability of the pulse top, including current ripple, is of the order of 0,1%.

The feed-back circuit (for beam current and for current in the winding) is not closed at the front and decay of the current pulse in the supplementary winding. In order to reduce the rise and decay time of the current pulse, the winding is supplied with voltages several times greater than the active component of the voltage drop in the winding. Shaping of the current pulse front begins at the moment when the 'start' pulse arrives from the accelerator's general timing system (fig.4). In this mode, the adjustment angle is close to zero, corresponding to a maximum voltage on the winding. Current decay is formed after the "stop" pulse has arrived from the general timing system. A constant adjustment angle, close to 150°, is set up in the phase control unit by means of the unit for switch-over to the inverter mode and this ensures optimum conditions for inverting the energy in the magnetic field of the supplementary winding. By reducing the rise and decay times of the current pulse to values several times smaller than the electromagnetic time constant of the circuit in the supplementary winding (0.2 sec.), the flat top can be efficiently used for multiple beam spill on several internal targets located at various azimuths.

4. Results

Fig. 6 shows an oscillogram illustrating the current variation in the supplementary winding (upper trace) which ensures a uniform spill intensity with a time lag of 800 millisec. at approximately 5% bunching (lower trace). In the current variation curve, the components with frequencies of 25-150 Hz, which compensate the magnet ripple, are clearly visible. An almost square form

for the variation of the extracted beams' intensity is ensured by high current variation rates at the first stage of beam spill. The mean value for secondary particle intensity does not vary by more than a few per cent throughout beam spill. The intensity rise time in the oscillogram in Fig. 6 is approximately 10 msec. and the decay time is approximately 30 msec.

Fig. 7a illustrates the deterioration of the time structure of extracted beam spill due to the effect of non-linear resonances. It can be seen that the disturbances of the proton beam caused by these resonances lead to up to 80% bunching of the secondary particle flux. Fig. 7b shows an oscillogram illustrating the improvement in beam spill on to the target obtained by introducing a field gradient correction which shifts the working point outside the range of non-linear resonances: the other targetting conditions remain the same as for the oscillogram in Fig. 7a.

Fig. 8 shows the oscillogram of a signal from the monitor during the successive extraction of secondary particles into two channels with time lags of 300 and 350 msec. The monitor was positioned so that it recorded secondary particles from both targets. It can be seen that the short rise and decay times. 10-15 msec., enable the length of the flat top to be used efficiently to operate several secondary particle channels in succession during one accelerating cycle.

Bibliography

1. G.S. Kazanskij, A.I. Mikhajlov, K.P. Myznikov, A.P. Tsarenkov. P.T.E. (Pribory i Tekhnika Eksperimenta) N°2, 1962.

2. K.P. Myznikov, I.N. Yalovoj. P.T.E. N°4, 1963.

3. K.H. Reich. Progress in Nuclear Technics and Instr. V. 11, 163, 1967.

4. V.I. Gridasov, K.P. Myznikov. IHEP Preprint 68-60, Serpukhov, 1968.

5. V.P. Shipillo. Avtomatizirovannyj ventil'nyj elektroprivod, (Automatically controlled drive converter), M., "Energiya", 1969.

The document was received by the publishing group on July 1970.

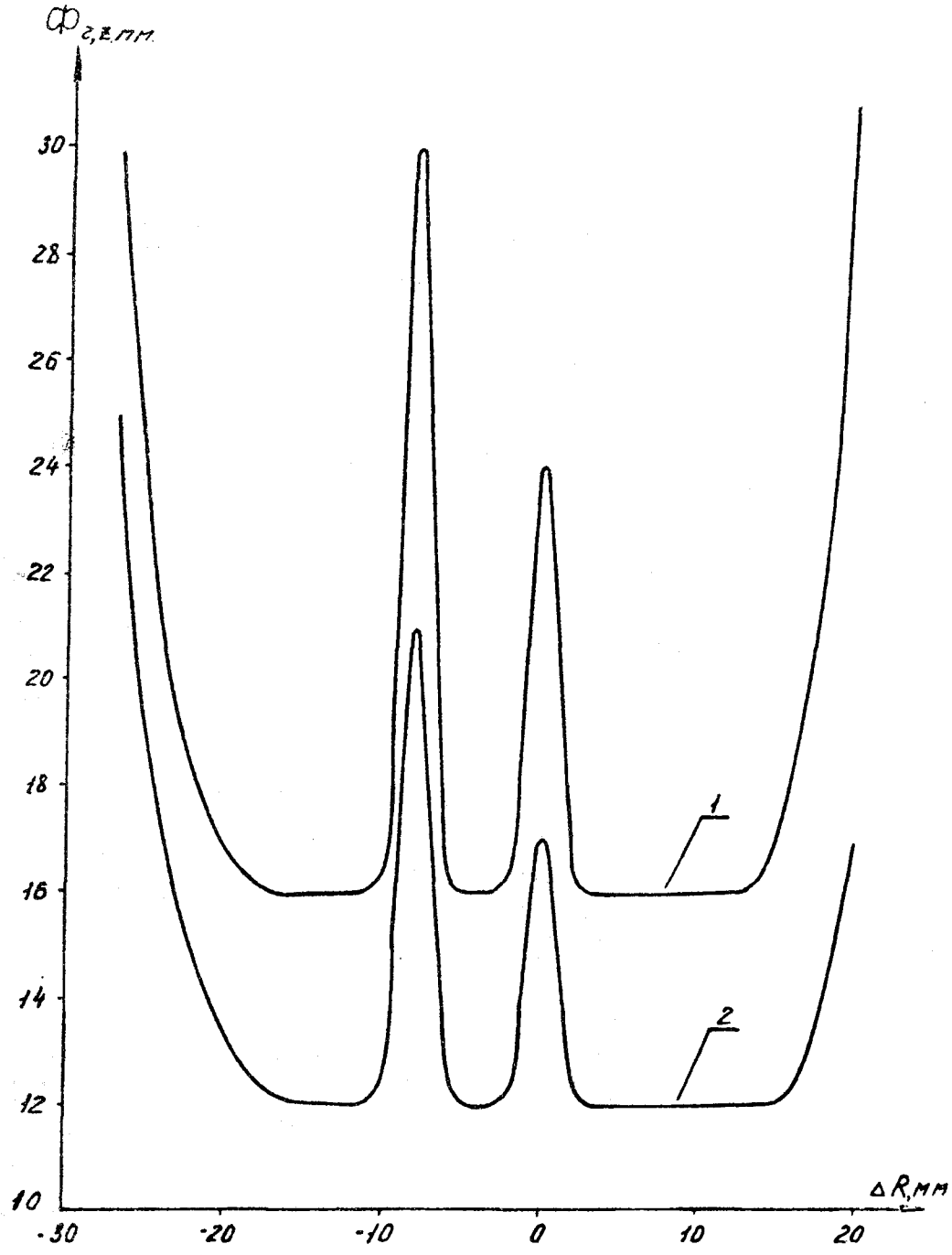

Fig. 1. Behaviour of the horizontal (curve 1) and vertical (curve 2) dimensions of the beam in motion at various radii during a flat top of H = 12 kOe in a radial focussing magnet.

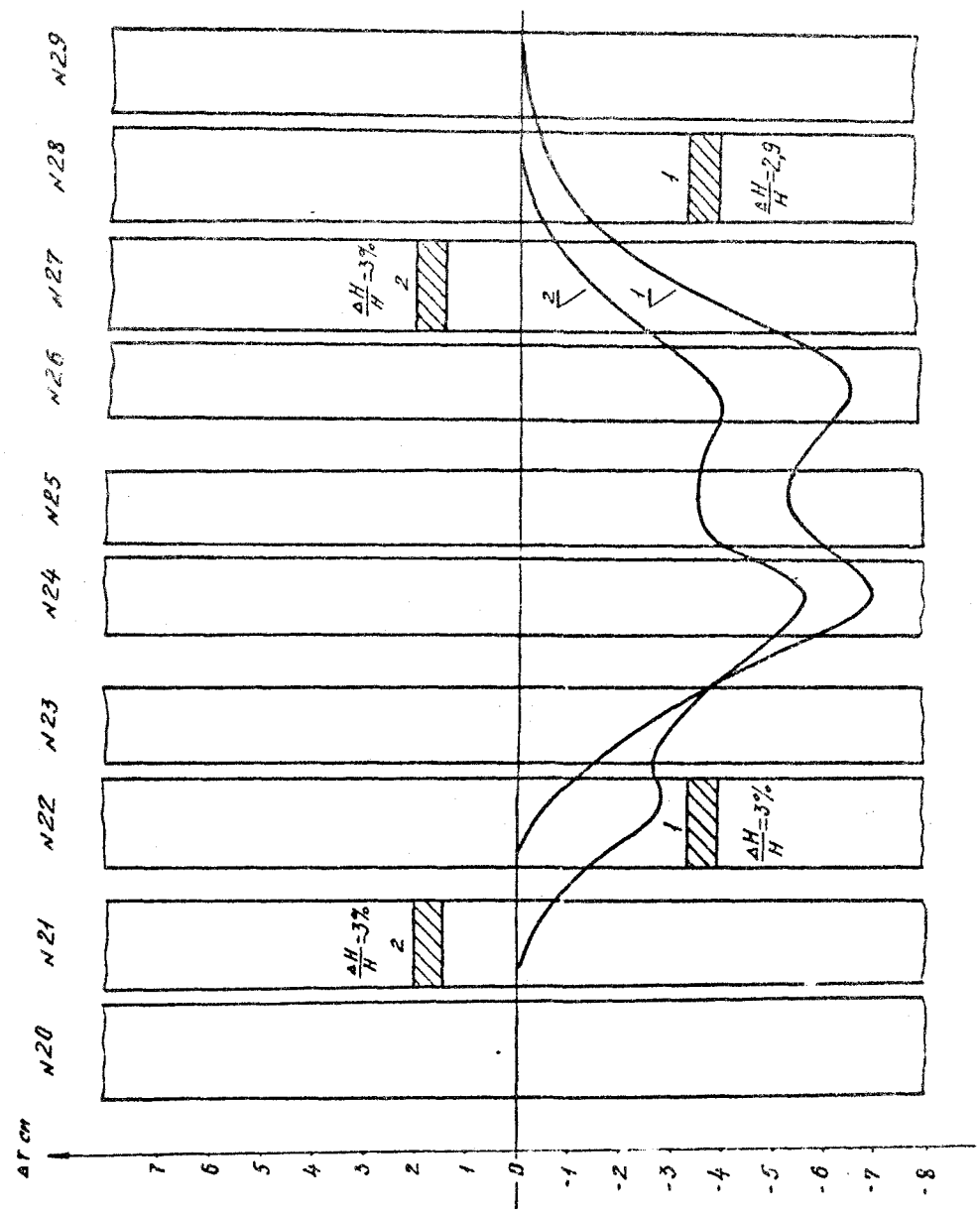

Fig. 2. Shape of the deformed orbit when azimuthal field asymmetry is excited in the focussing (curve 1) and defocussing (curve 2) units.

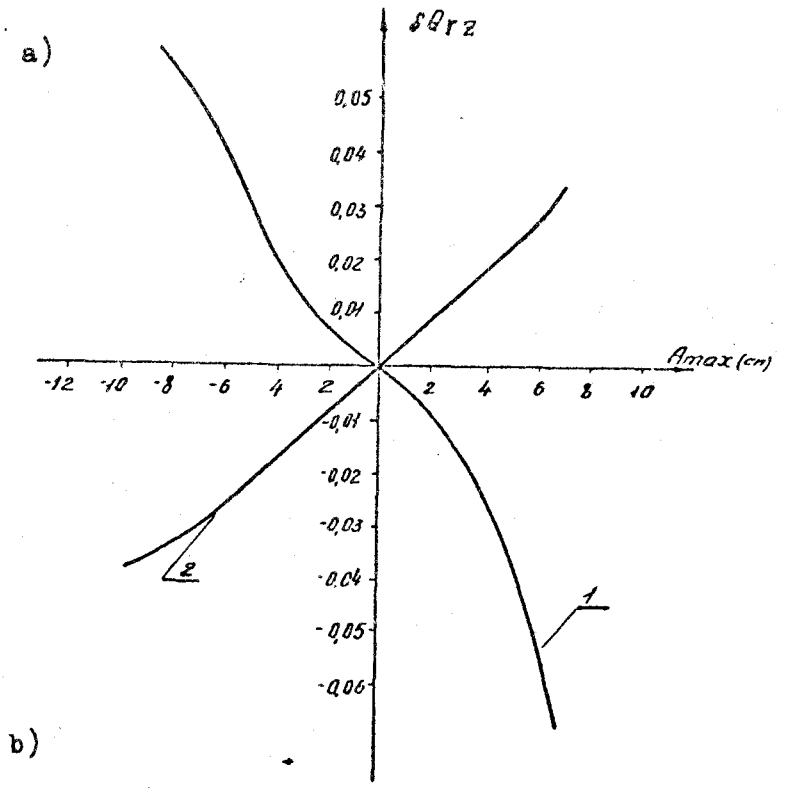

Fig. 3. Frequency shift of betatron horizontal (Curve 1) and vertical (curve 2) oscillations when azimuthal field asymmetry is excited in the focussing (case a) and defocussing (case b) units.

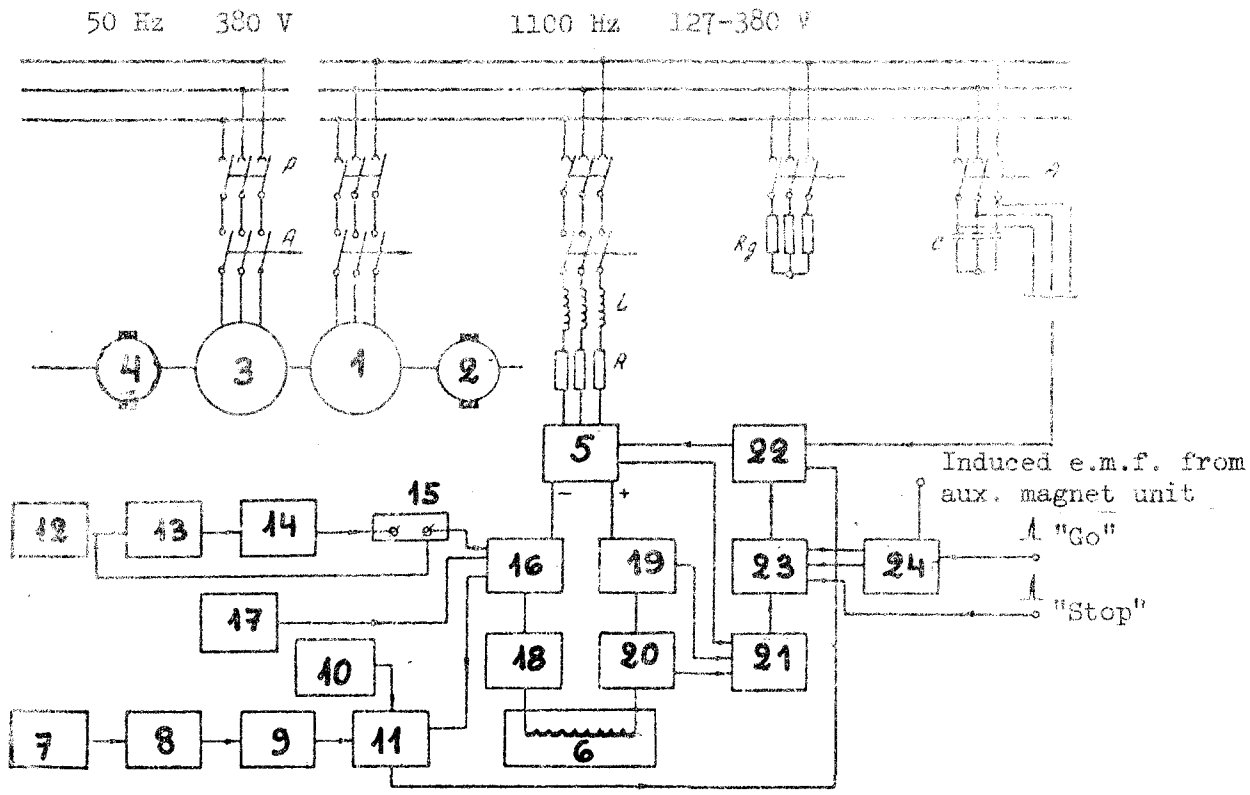

Fig. 4. Block diagram of the power supply system for the supplementary winding.

1. Synchro oscillator
2. Synchro oscillator driver
3. Synchro motor
4. Synchro motor driver
5. Controlled thyristor rectifier
6. Magnet unit's supplementary winding
7. Secondary particle intensity motor
8. Photomultiplier
9. Cathode follower
10. Reference voltage unit
11. Feed-back amplifier
12. Reference voltage pulse source
13. Direct current amplifier
14. Control transistor unit
15. Stabilizing shunt
16. Magnetic detector, of current
17. Power supply unit for magnetic current detector
18. D.C. current transducer for measurements
19. D.C. current transducer for protection
20. Pulse transducer for protection
21. Electron protection unit
22. Phase control unit
23. Unit for switch-over to inverter mode
24. Unit for controlling position of bump

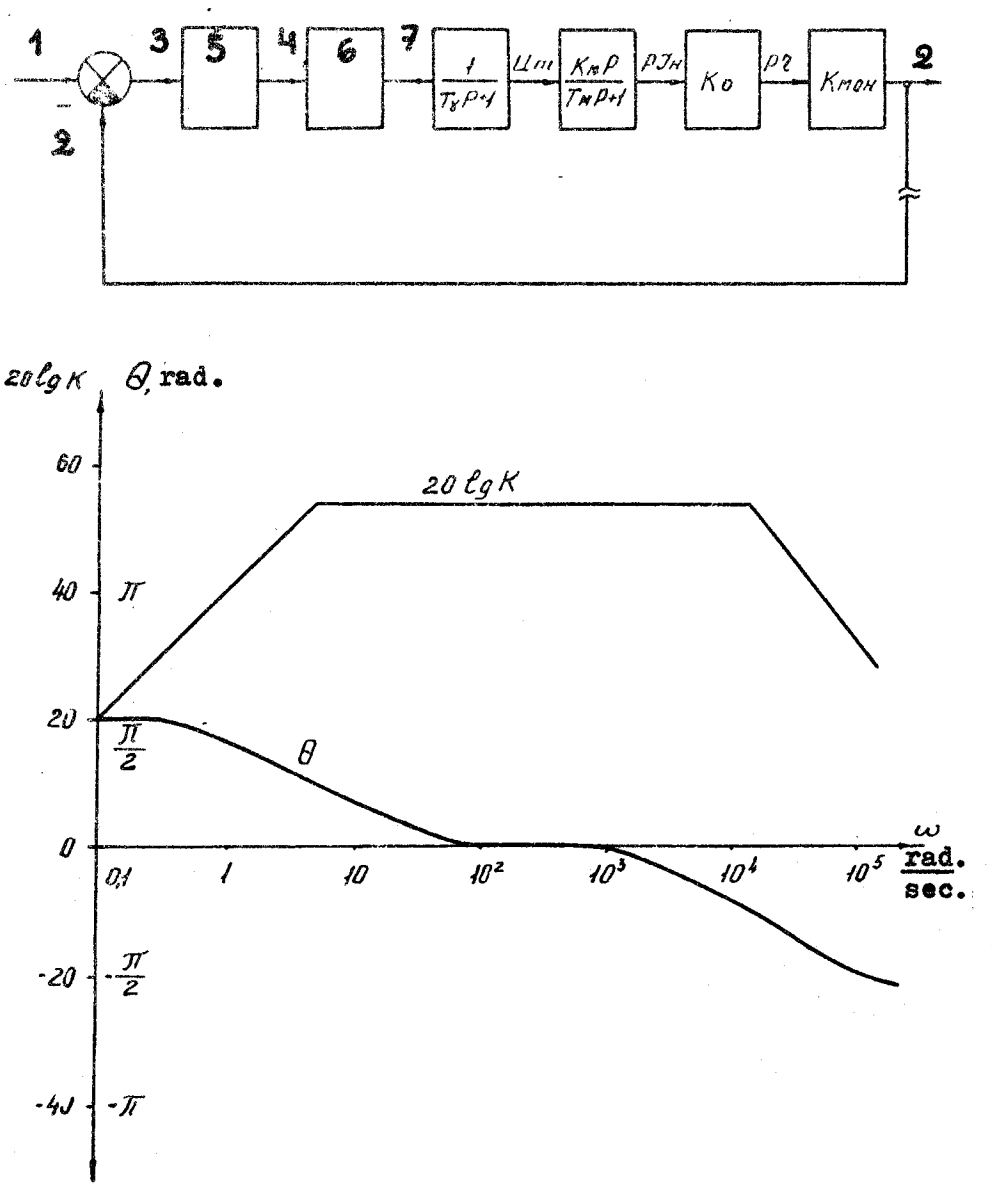

Fig. 5. Block diagram of the system for controlling beam current on to the target and the logarithmic frequency characteristics.

1. Operating circuit
2. Monitoring circuit
3. Input circuit
4. Output circuit
5. Feed-back amplifier
6. Controlled thyristor rectifier
7. Etc.

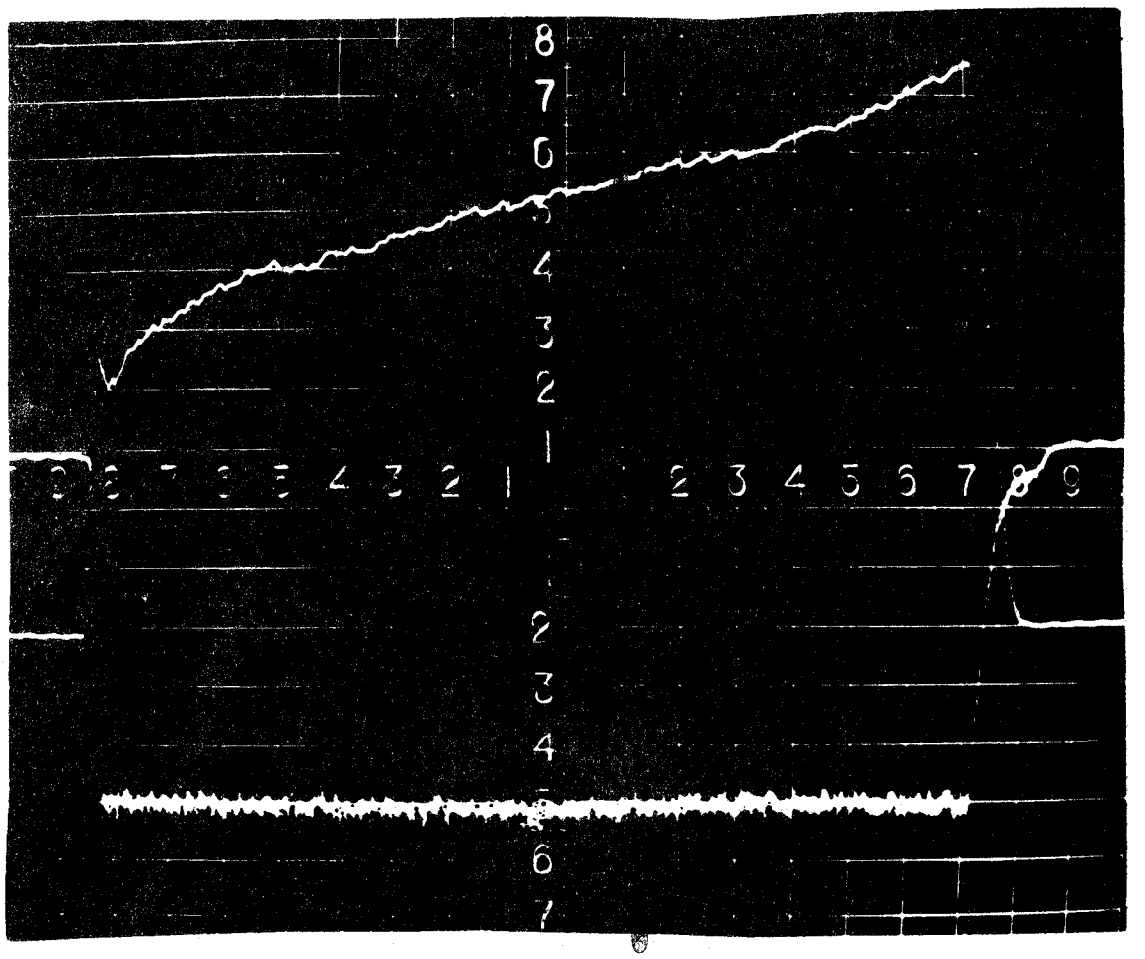

Fig. 6. Oscillogram of current in the supplementary winding (upper trace) and of the signal from the secondary particle intensity monitor (lower trace) during slow targetting. Sweep - 50 msec./square.

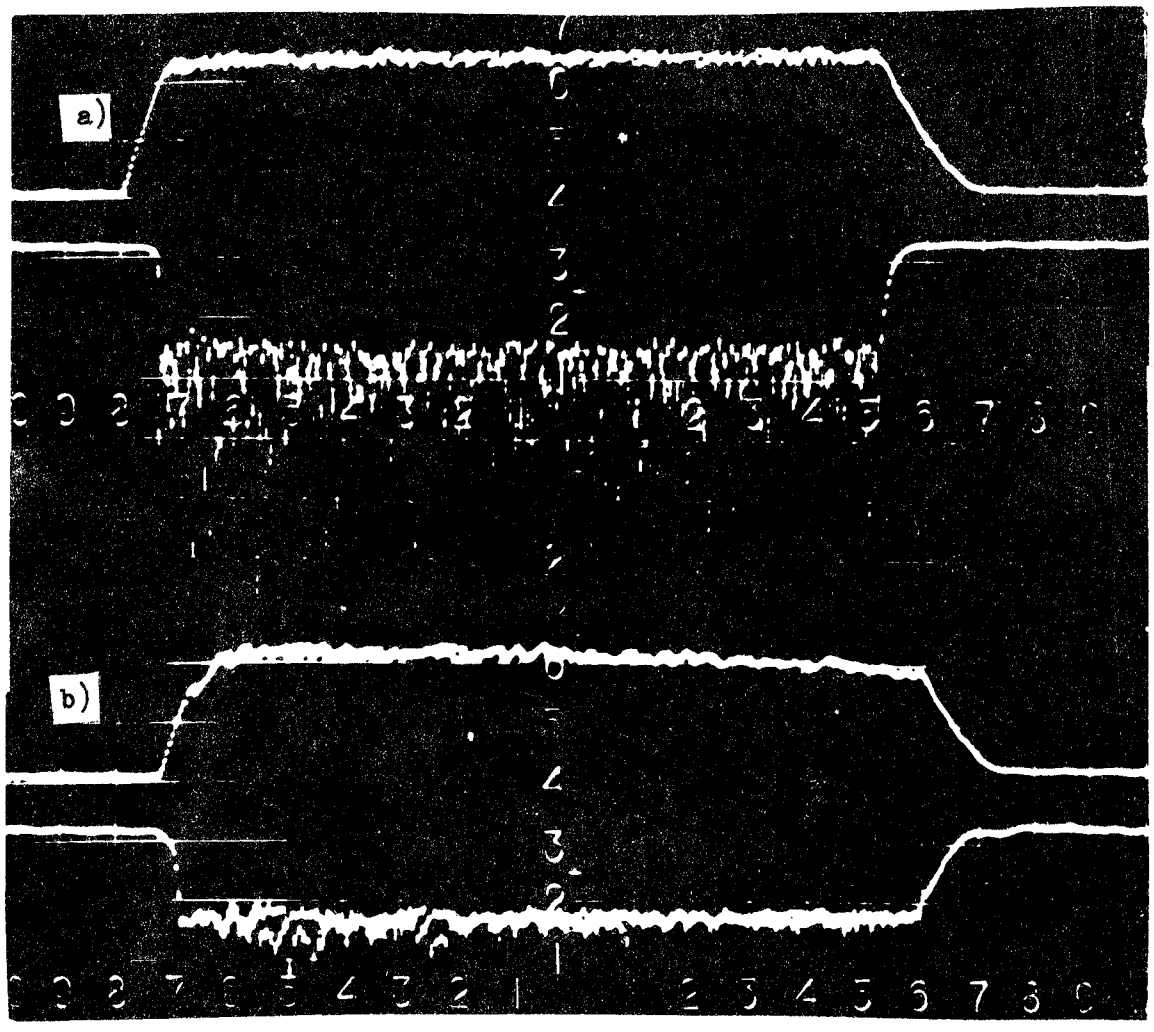

Fig. 7. Oscillograms of current in the supplementary winding and of signals from the secondary particle intensity monitor during slow targetting under the effect of non-linear resonances (a), and when they are suppressed (b). Sweep - 50 msec./square.

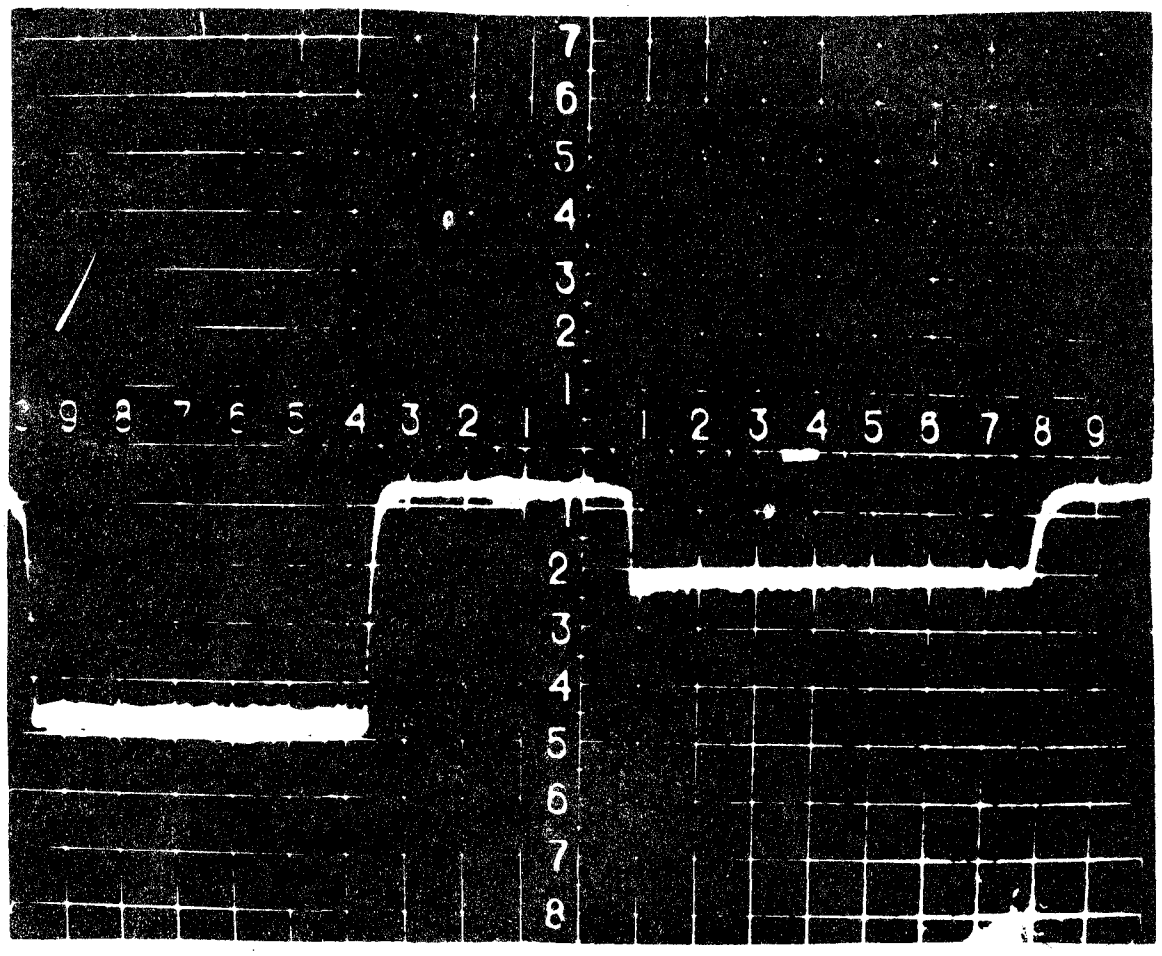

Fig. 8. Oscillogram of the signal from the secondary particle intensity monitor during successive slow targetting on to two targets in different channels. Sweep - 50 msec./ square.